Energy 89 (2015) 845–857

Contents lists available at ScienceDirect

Energy

journal homepage: www.elsevier.com/locate/energy

Effects of flue gas recirculation on the premixed oxy-methane flames in atmospheric condition

Yueh-Heng Li [a, b, *], Guan-Bang Chen [b], Yi-Chieh Lin [a], Yei-Chin Chao [a, **]

[a] Department of Aeronautics and Astronautics, National Cheng Kung University, Tainan, 701, Taiwan, ROC
[b] Research Center for Energy Technology and Strategy, National Cheng Kung University, Tainan, 701, Taiwan, ROC

ARTICLE INFO

Article history:
Received 11 January 2015
Received in revised form
6 June 2015
Accepted 9 June 2015
Available online 30 June 2015

Keywords:
Oxy-fuel
Oxy-combustion
Fluegas
Flame structure
Laminar burning velocity

ABSTRACT

This numerical study investigates the flame characteristics of premixed methane with various dilutions in order to simulate oxy-combustion of hydrocarbon fuels with flue gas recirculation system. In general, a recirculated flue gas consists of high concentration CO_2/H_2O and high gas temperature. The effect of various diluent gases on laminar burning velocity and adiabatic flame temperature is discussed via using Chemkin-pro simulation. By observing the resultant flame temperature and species concentration profiles one can identify that the flame front shifts, and the concentration profiles of major chemical reaction radicals varies, indicating the change of flame structure and flame chemical reaction paths. The dominant initial consumption reaction step of methane shifts from R53 ($H + CH_4 = CH_3 + H_2$) to R98 ($OH + CH_4 = CH_3 + H_2O$) when nitrogen is replaced by the recirculated gases. H and OH radical concentration would be influenced in various diluent gas cases, so that it leads to affect hydrogen formation and methane consumption. It is because that the chemical effects of the recirculated gases change the chemical reaction of the oxy-fuel combustion, and further affect reaction rate, species and radical concentrations.

1. Introduction

To curb the increasing GHG (greenhouse gas) emission, such as carbon dioxide (CO_2) and methane (CH_4), pertinent and promising implementations are proposed to achieve the mission of GHG emission mitigation. Several strategies for the reduction and capture of carbon dioxide from industrial power plants are being considered. In general, the carbon dioxide concentration in conventional coal-air combustion flue gas is low, so that its in-situ storage is not economically and practically feasible. The concept of combined oxy-fuel combustion recycling with CCS (carbon capture and sequestration) has been the most attentive scheme [1]. The oxy-fuel combustion is the method of using pure oxygen or a mixture of oxygen and recycled flue gas as an oxidant to generate the product gas composed of carbon dioxide and water steam near stoichiometric condition [2]. Theoretically, it enables to produce highly concentrated carbon dioxide flue gas through the water condensing treatment, and it has the potentials in reutilization and sequestration of carbon dioxide. Nowadays, to retrofit the traditional fossil fuel fired power plant for oxy-combustion has been considered one of the cost-effective and feasible implements [3,4] to promote this technology in industries.

Nevertheless, the difference in thermal properties of nitrogen and carbon dioxide results in significantly different flame behaviors of the oxy-fuel combustion from conventional air combustion [5]. Several studies have reported that the recirculated carbon dioxide participates in the chemical reaction instead of acting as an inert gas in oxy-enriched combustion. Indeed, carbon dioxide and water steam as diluent gas in hydrocarbon combustion would alter flame behaviors via the following three mechanisms: (a) dilution effect caused by the reduction in reactants concentration in the reactive mixture; (b) thermal effect due to the absorption of partial heat release by the diluents, leading to a change in flame temperature; (c) chemical effect due to the activity of the diluents that may alter some reactions pathways.

Wang et al. [6] numerically examined the combustion feature of pulverized coal in a CO_2/O_2 atmosphere over a range of CO_2-to-O_2 mole ratios between 2.23 and 3.65 in early stage. Kimura et al. [7] discovered that the ignition delay and flame instability would

* Corresponding author. Department of Aeronautics and Astronautics, National Cheng Kung Univ., Tainan, 701, Taiwan, ROC. Tel.: +886 6 2757575x63632; fax: +886 6 238 9940.
** Corresponding author. Tel.: +886 6 2757575x63690; fax: +886 6 238 9940.
E-mail addresses: yueheng@mail.ncku.edu.tw (Y.-H. Li), ycchao@mail.ncku.edu.tw (Y.-C. Chao).

http://dx.doi.org/10.1016/j.energy.2015.06.032
0360-5442/

occur in oxy-fuel combustion condition, and proposed that an increase of gas temperature and oxygen concentration in flue gas can mitigate the combustion instability. Besides, an increase of steam percentage in flue gas also can improve the oxy-fuel combustion efficiency. Ditaranto and Hals [8] stated that, in order to attain an adiabatic flame temperature similar to that in fuel-air combustion, oxygen volumetric concentration should be increased to at least 30% in their studies of CO_2/O_2 and methane premixed flame. Riaza et al. [9] mentioned that the ignition temperature was higher and the burnout velocity was lower in an atmospheric oxy-fuel condition ($21\%O_2 + 79\%CO_2$) than in air condition. This was due to the higher specific heat of CO_2 compared to N_2 and the lower diffusivity of O_2 in CO_2 than in N_2. Payne et al. [10] used a pilot-scale furnace to measure the gas emissions of oxy-combustion with dry and wet flue gas recirculation system. It is noted that the reduction of NO_x emission in dry flue gas recirculation system approached to 70% when the CO_2/O_2 mole fraction was 2.7. However, NO_x emission in wet flue gas recirculation decreased 83% when the $(CO_2 + H_2O)/O_2$ mole fraction was 3.2. In addition, the combustion efficiency of wet flue gas recirculation is higher than that of dry flue gas recirculation due to OH radical enhancement via H_2O pre-dissociation in a high temperature condition. Compared to nitrogen, the presence of carbon dioxide and water steam leads to an alteration of the chemical pathway. Haler et al. [11] experimentally and numerically investigated the flame behaviors of methane/air in different dilutions of CO_2, N_2, and CO_2–N_2 ($71.6\%N_2 + 28.4\%\ CO_2$). It was found that CO_2-dilution has inherently high thermal capacity compared to N_2-dilution, but also induces CO_2 dissociation.

Considered the effect of CO_2-dilution in chemical reaction of premixed hydrocarbon flames, Liu et al. [12] used fictitious carbon dioxide (CO_2(A)), which was artificially assumed to only possess identical thermal and transport properties as CO_2 but is excluded from chemical reactions, to compare with the real carbon dioxide results. It turned out that the flame burning velocity with fictitious CO_2(A) is lower than that with real CO_2. They attributed that CO_2 participates in the chemical reactions primarily through $CO_2 + H$═ $CO + OH$ (R99), and leads to reduction of laminar burning velocity. Corresponding to R99, significantly higher CO concentration was found in oxy-fuel combustion than in air combustion [13]. Park et al. [14] studied the effects of CO_2 dilution on methane-air flames and concluded that the addition of CO_2 influences the chemical flame structure. Similarly, Mazas et al. [15] investigated the effects of water steam addition on the laminar burning velocity of oxygen-enriched methane flames. It was found that water steam addition has a significant chemical effect on the burning velocity of methane-air flames, especially in lean and near-stoichiometric conditions.

Accordingly, the existence of recirculated carbon dioxide and water steam in oxy-fuel combustion certainly would induce chemical effect of premixed flame and modify flame characteristics and structure. Parameters, such as flue gas recirculation ratio, flue gas temperature as well as flue gas contents, are engaged to influence oxy-enriched and oxy-fuel combustion characteristics. These parameters are crucial in the design of oxy-enriched or oxy-fuel combustor. Although there is considerable literature on oxy-fuel combustion, systematic studies of physical and chemical flame structures of the oxy-fuel combustion under various flue gas recirculation conditions have not been reported and documented. This study would numerically examine the effects of flue gas additions on key flame characteristics, such as adiabatic flame temperature and flame burning velocity of methane/oxygen-flue gas combustion as compared with methane/air combustion, to distinct the role of the recirculated flue gas in oxy-fuel combustion. Various recirculation ratios of nitrogen, carbon dioxide, water steam, and flue gas ($33\%CO_2 + 67\%H_2O$) dilution in oxy-methane premixed combustion are numerically considered. The flame structures of methane/air premixed combustion in various flue gas dilutions are also investigated to serve as the baseline data for comparison.

2. Methodology

For studies of the chemical effects of oxy-fuel combustion, numerical simulation is a cost-effective and high-performance implement to observe the insight of flame structure and flame characteristics. Among currently available numerical mechanisms, GRI-Mech. 3.0 is extensively and intensively used in numerical analysis of oxy-methane combustion. For instance, Liu et al. [12] numerically investigated the chemical effects of carbon dioxide in oxy-fuel condition via GRI-Mech. 3.0. Mazas et al. [15] numerically investigated the effects of water steam addition on the laminar burning velocity of oxygen-enriched methane flames using GRI-Mech. 3.0, while Watanabe et al. [16] used GRI-Mech. 3.0 to examine the NOx formation and reduction mechanisms in staged oxy-fuel combustion and in air combustion. However, a modified GRI-Mech 3.0 is sometime applied in specific researches of oxy-fuel combustion. Watanabe et al. [17] used the modified GRI-Mech 3.0 [18] to discuss the impact of carbon dioxide on methane oxidation and hydrogen formation in fuel-rich oxy-combustion. The modified GRI-Mech. 3.0 involves 97 species and 779 elementary reactions that are larger than those in original GRI-Mech. 3.0. Abián et al. [19] used another modified mechanism, which consists of 128 species and 924 elementary reactions [20], to observe the impact of CO_2 and H_2O concentration on the oxidation process of CO. Nonetheless, the modified GRI-Mech 3.0 with larger species and reaction steps is usually designed and optimized for specific purpose and is generally more time-consuming and numerically unstable compared with GRI-Mech. 3.0. In this study, for general comparisons of the different oxy-methane and methane-air combustions with various flue gas dilution conditions, the unmodified GRI-Mech. 3.0 will be used with proper validations in the oxy-fuel combustion simulation.

2.1. Numerical methods

The PREMIX code of CHEMKIN Collection is used to calculate the adiabatic, unstrained, free propagation velocities of the CH_4 laminar premixed flames. It solves the equations governing steady, isobaric, quasi-one-dimensional flame propagation. For a freely propagating flame, the mass flow rate is an eigenvalue and must be determined as part of the solution. To obtain the accurate flame speed, the boundaries should be sufficiently far from the flame to avoid temperature and species gradients at the boundaries. In addition, the adiabatic flame temperature is calculated by using the EQUIL code of CHEMKIN Collection. An initial reactant mixture is specified and equilibrium of constant enthalpy and constant pressure is constrained.

As to the chemical kinetics, the GRI-Mech 3.0 mechanism [21] composing of 53 chemical species and 325 reaction steps and detailed transport properties are used. The reaction rate constant is represented by the modified Arrhenius expression,

$$k = \overline{A}T^b \exp\left(\frac{-E_a}{RT}\right) \tag{1}$$

where $\overline{A}$ is the pre-exponential factor, b is the temperature exponent, and E_a is the activation energy. The chemical kinetics with CHEMKIN format is used in the code. Details of the chemical reaction rate formulation and CHEMKIN format can be found in the user's manual [22].

At the cold boundary, the temperature of unburned reactants is 400 K. The effects of different diluents (N_2, CO_2, H_2O or flue gas) on CH_4 laminar burning velocity are investigated. The composition of flu gas is 33% CO_2 and 67% H_2O. The global reaction of CH_4/O_2/diluents is defined as:

$$\varphi CH_4 + 2(O_2 + \gamma D_i) \rightarrow CO_2 + 2H_2O + 2\gamma D_i \quad (2)$$

where φ is the equivalence ratio and D_i the diluents. The dilution ratio γ is defined as the mole ratio of diluents with respect to oxidizer, while the RR (recirculation ratio) is defined as the ratio of mole fraction between diluents and oxidizer.

2.2. Flame speed measurement methodology

In order to validate the accuracy of applying GRI-Mech 3.0 in oxy-fuel combustion simulation, experimental and numerical laminar burning velocities in various flue gas dilutions are performed and compared. The laminar burning velocity (s_u^o) is the velocity at which a laminar, steady, unstretched, adiabatic flame moves relative to the unburned premixed gas in the direction normal to the flame surface, and it implicates physical and chemical properties of flames. However, it is difficult to produce a perfect flame which confirms all requirements for measuring laminar burning velocity. Various configurations and contraptions were proposed and developed to generate flows approaching these conditions and eliminate the thermal, stretch and curvature effects which are known to influence the laminar burning velocity [23]. A rim-stabilized conical flame is a practical and reliable implement used to experimentally determine the laminar burning velocity for laminar premixed oxy-fuel flame studies [24,25]. According to mass balance equation of conical flame, the area-weighted average laminar flame speed (s_u) is given:

$$\dot{m} = \rho_u \times s_u \times A_f$$

where $\dot{m}$ is the reactant mass flow rate, ρ_u the unburned gas density and A_f the flame surface area. The appropriate flame surface indicates the upstream boundary of preheat zone, and it can be determined from the Schlieren images with an edge detection technique. The steady adiabatic unstretched laminar flame speed can be determined by performing the correction derived by Sun et al. [26].

$$\frac{s_u}{s_u^o} = 1 + \frac{Ze}{2}\left(\frac{1}{Le} - 1\right)\frac{\alpha^o \kappa \delta_T^o}{s_u^o} + c\delta_T^o$$

where Ze is the Zeldovitch number, *Le* the Lewis number of the reactive mixture, κ the global stretch rate, δ_T^o the thermal flame thickness, c the flame curvature and α_o a factor accounting for the thermal expansion effect. The above parametric quantities can be extracted from numerical simulations of one-dimensional adiabatic unstretched flames using the procedure suggested in Ref. [15] and Ref. [26]. Ultimately, the laminar burning velocity (s_u^o) of conical flame in various flue gas dilutions can be determined.

2.3. Experimental apparatus and validation

Fig. 1 shows the sketch of experimental set-up. Methane, oxygen, carbon dioxide and nitrogen gases are individually supplied from pressurized tanks. The flow rates are regulated with mass flow controllers (5850E, Brooks Instrument), calibrated with the dry flow calibrator (Definder 220, Bios). The uncertainty of mass flow rates is within 1%. The heater with controller (SH01 & TRC202, T.S.K) is used to evaporate water and preheat up the mixtures. The mixture (oxygen + diluent gas) and the methane flow are premixed before being introduced in an axisymmetric burner. The reactive mixture successively flows through a perforated plat, a honeycomb structure and a metallic grid to obtain a laminar flow entering the inlet of a profiled converging nozzle. The converging nozzle is used to reduce the boundary layer thickness by accelerating the flow and to obtain a top-hat velocity profile at the burner outlet. The diameter of burner is 7 mm. The Schlieren technique is used to determine the flame area. For each operating condition, 20 Schlieren images are recorded and the corresponding root-mean-square deviation of the flame surface area is less than 2% of the mean flame area.

The numerical and experimental laminar burning velocity of premixed oxy-methane flames in various recirculating flue gas conditions are plotted with various recirculation ratios in Fig. 2. The RR (recirculation ratio) is the ratio of diluent flow rate and oxygen flow rate. It turns out that experimental results are consistent with numerical results within 1.5% of discrepancy, so that the validation of using GRI-Mech. 3.0 mechanism in various recirculation ratios of oxy-fuel combustion is proved to be acceptable. As to steam addition in oxy-combustion, it had been shown and verified by Mazas et al. [15].

3. Results and discussion

3.1. Adiabatic flame temperature and laminar burning velocity

Investigations of the effects of diluent gas on oxy-methane flame behaviors, started with the adiabatic flame temperature and laminar burning velocity of premixed methane flame and the results versus various recirculation ratios ranging from 0.25 to 3 are shown in Fig. 3 as the baseline data for further comparison and analysis. The dash lines in Fig. 3 indicate the numerical results of fictitious chemically-inert gases which do not engage in chemical reactions in flames. Results show that N_2-diluent case has largest adiabatic flame temperatures and laminar burning velocities, while CO_2-diluent case has lowest values. The difference of adiabatic flame temperature among various dilutions becomes significant with increase of recirculation ratios. The reason is that the heat capacity of CO_2 (37 J/mol·K) and H_2O (33 J/mol·K) is higher than that of N_2 (21 J/mol·K), and it contributes to reduction of the flame temperature in the high recirculation ratios. On the contrary, when recirculation ratio goes smaller, namely in high oxygen concentration condition, the difference of flame temperature among various dilutions becomes smaller. It is due that oxygen-rich combustion apparently induces high flame temperatures of flue gas, and reduces the thermal effect of diluent gas with individual heat capacity. It is interesting to note that the adiabatic flame temperatures of CO_2-dilution with RR of 2.2, H_2O-dilution with RR of 2.9 and fluegas-dilution with RR of 2.65 are analogous with that of stoichiometric methane/air flame (RR = 3.76). It has been shown in the literature that oxy-methane flame with CO_2-dilution requires higher oxygen concentration to maintain the combustion temperature of stoichiometric methane/air flame, especially when retrofitting the plant. In addition, the difference of adiabatic flame temperature between the fictitious chemically-inert gases and the real diluent gas are not significant in cases of high recirculation ratio. It confirms that heat capacity of diluent gas is the primary contributor to influence the change of oxy-methane flame temperature in various dilutions. However, the adiabatic flame temperature between the fictitious and real diluent gas has obvious differences in cases of low recirculation ratio, since the thermal effect is not the sole key contributors in the high oxygen concentration condition.

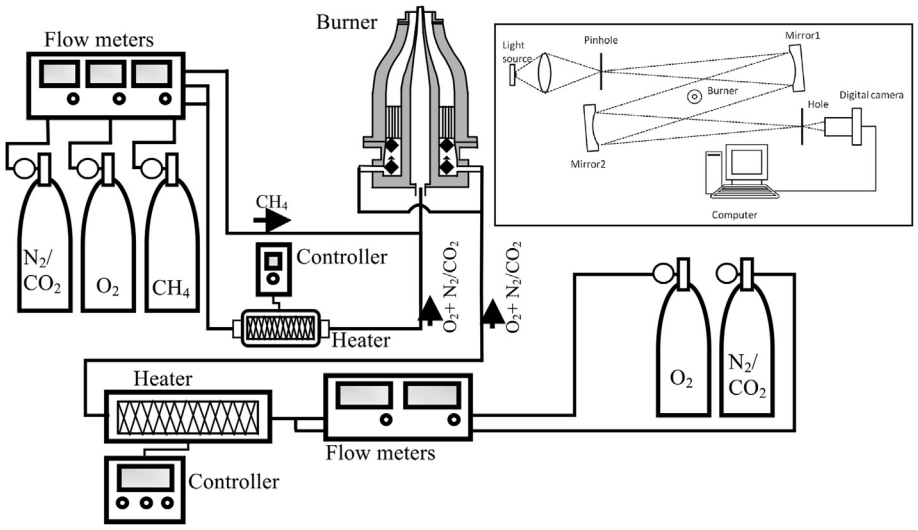

Fig. 1. Schematic diagram of experimental setup.

In the case of RR = 2 the laminar burning velocity of N_2-dilution (1.5 m/sec) is much higher than that of CO_2- (0.39 m/sec), H_2O- (1.06 m/sec) and fluegas-dilution (0.77 m/sec). As shown in Fig. 3b, the difference of laminar burning velocity in various dilutions firstly increases and then decreases with an increase of the recirculation ratio. The maximum difference of laminar burning velocity among various dilutions occurs in the vicinity of RR = 1.0. Compared with Fig. 3a, the flame temperature difference among various dilutions is insignificant at RR = 1, but flame speed difference is not. This implies that the effect of diluent gas on flame speed is not only affected by heat capacity of diluent gas, but also by other chemical properties of diluent gas. Furthermore, compared with the burning velocities of the fictitious cases CO_2(A)- (0.757 m/sec), H_2O(A)- (1.293 m/sec) and fluegas(A)-dilution (1.086 m/sec) in the condition of RR = 2, the burning velocities for the real diluent gas dilution cases are found significantly lower. Presumably, flue gas recirculation does not only contribute as an inert to the thermal effect of the flame and the burning velocity, but also significantly involved in the chemical effect affecting the flame burning velocity.

It is of interest to note that the maximum difference of adiabatic flame temperature in various dilutions occurs in high recirculation ratios, and it can say that increasing amount of diluent gas will amplify the thermal effect of diluent gas on the flame temperatures according to the individual heat capacity. As the recirculation ratio is decreased, the amount of dilution in oxy-methane combustion is correspondingly decreased. The contribution due to thermal effect of diluent gas will be spontaneously reduced. The result in Fig. 3a shows the decreasing difference of adiabatic flame temperature between nitrogen dilution and the other dilutions. However, the

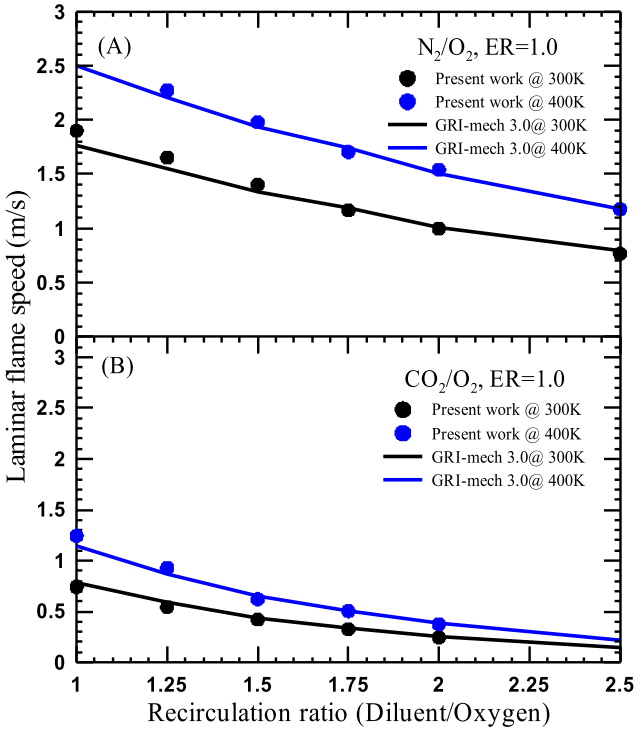

Fig. 2. Numerical and experimental laminar flame speed in various recirculation ratios.

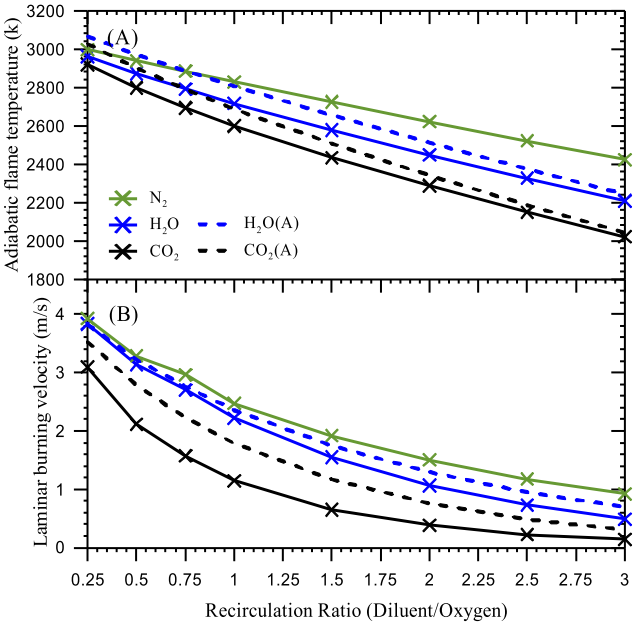

Fig. 3. Adiabatic flame temperature and laminar burning velocity of methane premixed flame in various recirculation ratios.

maximum difference of laminar burning velocity in various diluent gas occurs at the RR = 1 condition with equal amount of oxygen and diluent gas. The effect of diluent gas on flame speed should be theoretically reduced due to decreasing diluent gas concentration, but high-temperature environment forces carbon dioxide and water steam to participate in chemical reaction of the flames. It leads to the chemical effect of carbon dioxide and water steam emerging and being dominant in low recirculation ratios. In order to further understand the role of diluent gas in oxy-methane combustion, the moderate recirculation ratio is selected at RR = 2.0 to examine the existing effects happening to flame temperature and flame speed.

3.2. The sensitivity analysis of flame speed

To further look into chemical effects of various diluents on flame speed, the sensitivity analysis of flame speed for four dilution cases with inlet gas temperature of 400 K and recirculation ratio of 2 is performed. The results are shown in Fig. 4 that the chain branching step R38 ($O_2 + H{=}O + OH$) is the primary contributor reaction step in oxy-methane premixed combustion, and it is also the principal source of radical production to accelerate the chemical reactions. The secondary contributor reaction step for all cases is R52 ($H + CH_3 + M{=}CH_4 + M$), which is the initiation reaction of methane oxidation in low temperature environment. Unlike energetic fuel or strong oxidizer addition [27] in hydrocarbon fuel, that overwhelmingly alters the chemical pathway of radical production, diluents in oxy-methane combustion will not alter the dominant reaction steps contributing to the flame speed. The third reaction step in cases of N_2-, H_2O-, CO_2(A)-, H_2O(A)- and fluegas(A)-dilution is R99 ($OH + CO{=}H + CO_2$), which is the principal reaction step of carbon monoxide oxidation and primary exothermicity in methane combustion. However, in cases of CO_2- and fluegas-dilution the third important reaction step will change to R119 ($HO_2 + CH_3{=}OH + CH_2O$), which is the principal reaction step of CH_3 oxidation reaction. In particular, CO_2 dilution in oxy-methane combustion will not alter the chemical pathway of primary radical production, but enhance the importance of reaction branch step of methane oxidation. On the contrary, in H_2O-dilution oxy-methane combustion the priority of chemical reactions affecting flame speed is similar to that in N_2-dilution case.

3.3. The analysis of flame chemical structure

In the following analysis of the chemical structure of the oxy-methane flame with dilutions the conditions considered for the four dilution cases are the inlet gas temperature of 400 K and recirculation ratio of 2. PREMIX code of CHEMKIN collection 3.5 is used for analyzing the flame structure of premixed oxy-methane combustion. In the analysis, the first step is to calculate and plot the concentration distributions of the main species in the flame. Then, the second step is further to examine the dominant chemical reactions and to construct reaction pathway in the reaction zone of the flame. Ultimately, it can help to delineate the chemical effects of dilution gas additions on premixed oxy-methane flames.

3.3.1. N_2-dilution air-methane flame

In Fig. 5, it shows the distributions of main species and radical concentrations along the axial direction of the N_2-dilution air-methane flames at 400 K of inlet gas temperature and RR = 2.

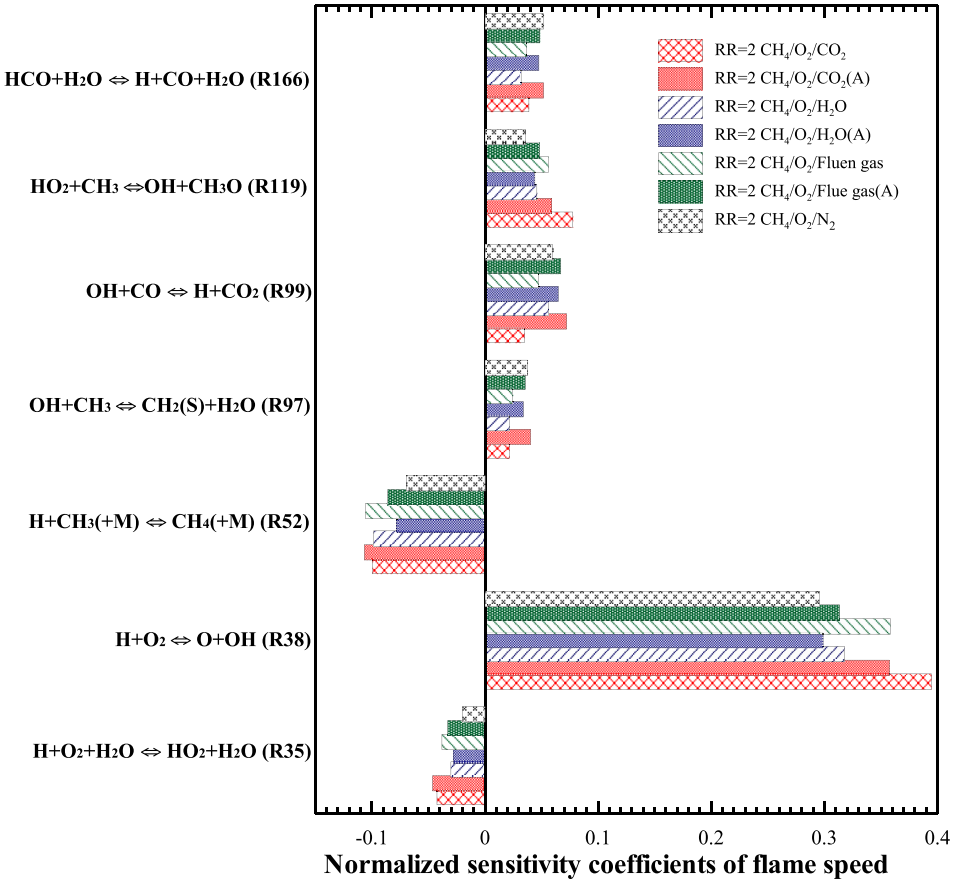

Fig. 4. The sensitivity analysis of laminar burning velocity with respect to different chemical reactions.

The vertical dash line represents the location of methane auto-ignition temperature (868 K), which is defined as the location of flame front. For convenience of analysis and comparison of the numerical results, the vertical dash line, the methane auto-ignition temperature, is used to separate the preheat and reaction zone of the flame. The preheat zone is defined as the area between the onset of reactant consumption and the location of methane auto-ignition temperature (left hand side of the vertical dash line). The reaction zone defined as the area behind the location of methane auto-ignition temperature with distributions of numerous major reaction radicals on the right hand side of the vertical dash line. Tracking the history of species and radical concentrations along the direction of the flame coordinate, it is significant to find the initial consumption of methane and oxygen, and production of hydrogen and few intermediates, such as CH_3 and HO_2, in the preheat zone. Once entering reaction zone, a significant increase in the production of H_2, CO and above-mentioned intermediates until the complete consumption of methane can be observed. Accompanying with emerging radical productions (such as O, H and OH), it is to accelerate H_2 and CO consumptions and produce the resultant products of H_2O and CO_2.

Fig. 6 shows the simplified methane oxidation mechanism in N_2-dilution air-methane environment. The main chain branching reactions of OH radical production are R3 ($O + H_2 = H + OH$) and R38 ($O_2 + H = O + OH$), while main reactions of H radical production are R10 ($O + CH_3 = H + CH_2O$) and R84 ($OH + H_2 = H + H_2O$). However, the rate of R38 is higher than that of R3, and the rate of R84 is higher than that of R10, as shown in Fig. 7. In general, the H and OH radicals trigger initial methane hydrogen abstraction through R53 ($H + CH_4 = CH_3 + H_2$) and R98 ($OH + CH_4 = CH_3 + H_2O$) to form CH_3 for further oxidation. The rate of R53 is significantly higher than that of R98 in N_2-dilution air-methane combustion, as shown in Fig. 7. However, the methane oxidation follows the three major routes through CH_2O or CH_2 and the recombination of CH_3

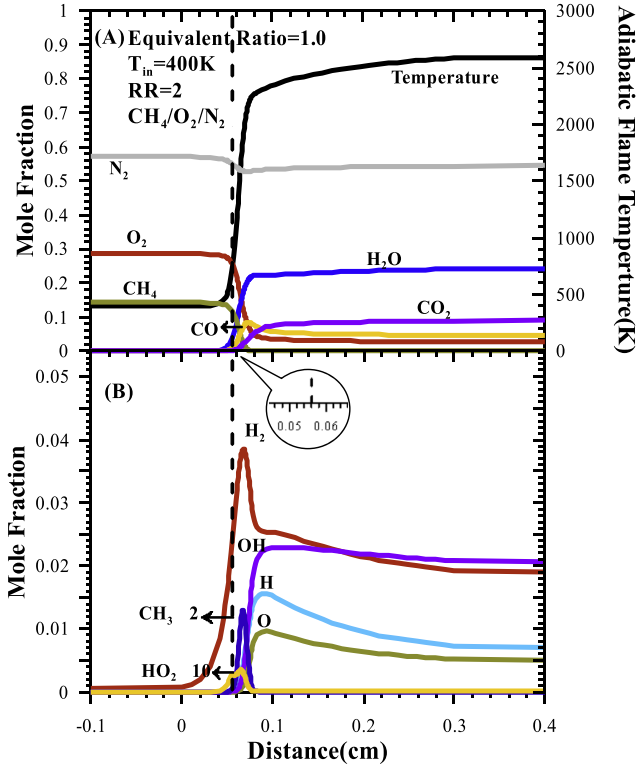

Fig. 5. Species concentration distribution $CH_4/O_2/H_2O$ at RR = 2 and T_{in} = 400 K.

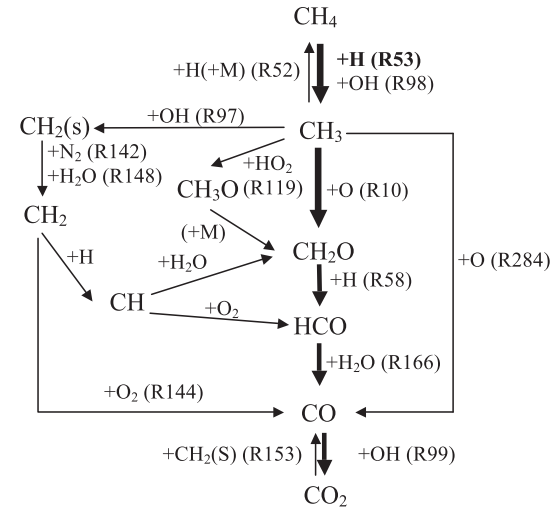

Fig. 6. Simplified methane oxidation mechanism in N_2-dilution oxy-fuel environment.

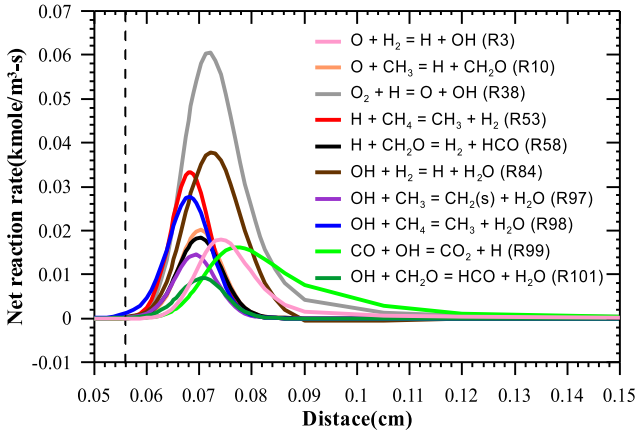

Fig. 7. The net reaction rate of $CH_4/O_2/N_2$ at RR = 2 and T_{in} = 400 K.

[28]. CH_3 may be consumed through R10 ($O + CH_3 = H + CH_2O$) with production of CH_2O or through R97 ($OH + CH_3 = CH_2(s) + H_2O$) with production of CH_2, and recombined to CH_4 via R52 ($H + CH_3 + M = CH_4 + M$, M: third body). Comparing net reaction rate of these reactions, the rate of R10 is higher than that of R97 and R52, indicating the dominant route of methane oxidation through CH_2O in N_2-dilution flame.

Besides, CH_2O is mainly consumed through R58 ($H + CH_2O = H_2 + HCO$) and R101 ($OH + CH_2O = HCO + H_2O$), and produces HCO. The rate of R58 is higher thant that of R101, as shown in Fig. 7. Then, HCO is mainly consumed through R166 ($HCO + H_2O = H + CO + H_2O$). CO is consumed through R99 ($CO + OH = CO_2 + H$) and eneventually yeilds CO_2 in the end. However, the chemical reactions of CO production could be from R144 ($O_2 + CH_2(S) = H + OH + CO$) and R153 ($CO_2 + CH_2(S) = CO + CH_2O$) through CH_2, R284 ($O + CH_3 = H + H_2 + CO$) through CH_3, and the backforward direction of R99.

3.3.2. H_2O-dilution oxy-methane flame

Fig. 8 shows the distribution of main species and radical concentration along the axial direction in H_2O(A)- and H_2O-dilution oxy-methane flames at 400 K of gas temperature and RR = 2. In H_2O(A)-dilution case, it is only concerned with the thermal effect of dilution on the flame structure. It turns out that the locations of

flame front in N_2- and H_2O(A)-dilution cases are analogous, and the trends and profiles of species and radical concentrations in both cases are approximately consistent. The main differences between these two cases are the flame temperature and radical concentrations, as shown in Fig. 5, Fig. 8a and b. The concentrations of all radicals in Fig. 8b are reduced due to low flame temperature. It is generally expected that the thermal effect of diluent gas only impacts on the flame temperature and reaction kinetics, but not involves in chemical reaction. Comparing profiles of species and radical concentrations in H_2O(A)- and H_2O-dilution cases, the locations of flame front are apparently identical, and the location of H_2O-dilution case slightly moves downstream. Besides, the concentrations of H_2 and some radicals, such as OH and HO_2, are apparently increasing in H_2O-dilution case, but the concentrations of CO and other radicals, such as CH_3, O and H, are reducing. It is of interest to note that the concentration of HO_2 in preheat zone significantly increases, and the slope of CH_4 consumption becomes smoother in the H_2O-dilution environment compared to that in the N_2-dilution environment. Furthermore, the amount of H_2 is increasing obviously, and its peak profile decays slower, especially in the trailing edge of the flame and the post flame regions, than that in H_2O(A)- and N_2-dilution environments. As the axial diffusion is included in the numerical calculation of the premixed flame mode, the hydrogen and radical distributions become wider than the other species due to their high thermal diffusivities.

Fig. 9 shows the production rate of species and radicals in N_2- and H_2O-dilution oxy-fuel flame at the location of flame front. It is obvious that the methane and oxygen consumption rates and the hydrogen and CO production rates in H_2O-dilution environment

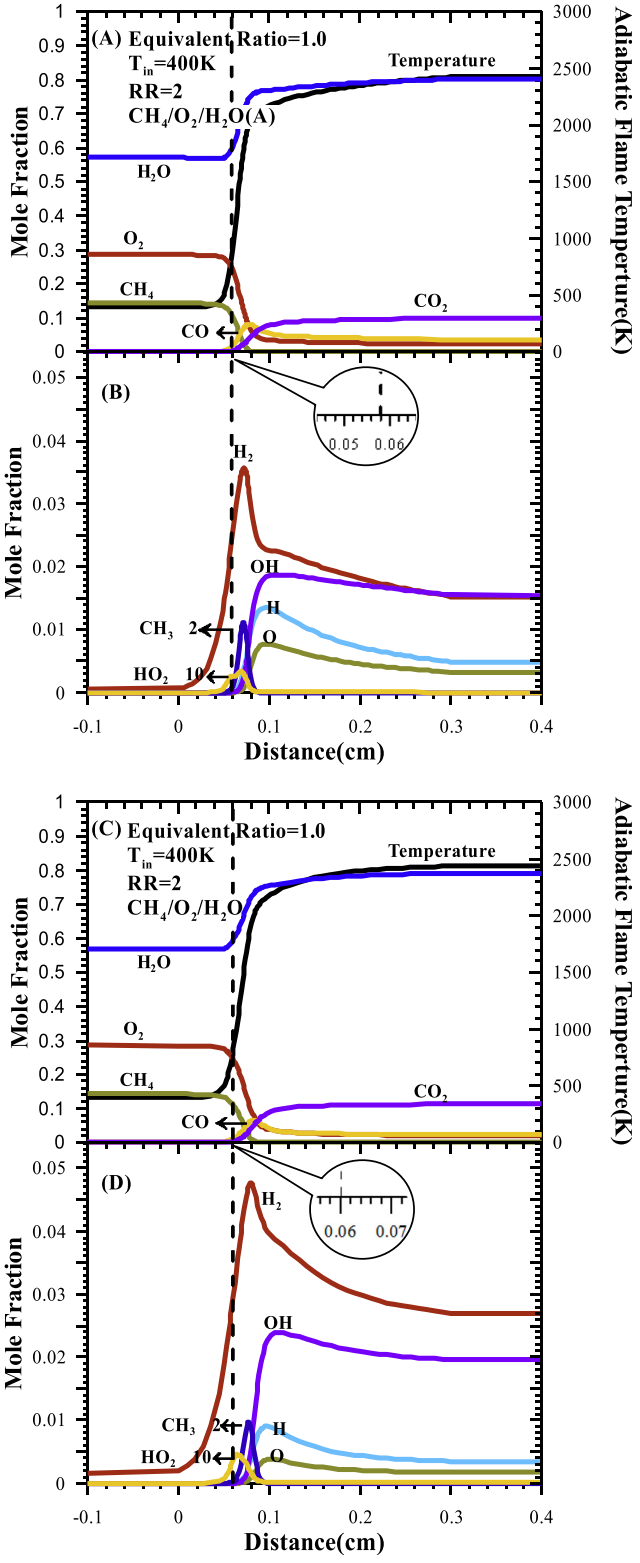

Fig. 8. Species concentration distribution of (a, b) $CH_4/O_2/H_2O$(A) and (c, d) $CH_4/O_2/H_2O$ at RR = 2 and T_{in} = 400 K.

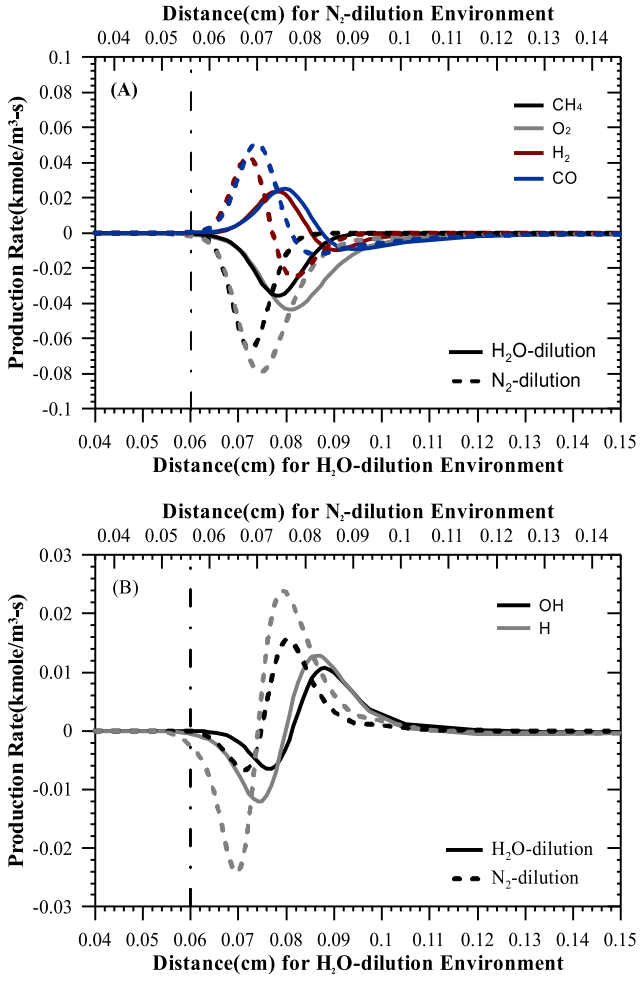

Fig. 9. The production rate of Species and radical of $CH_4/O_2/N_2$ and $CH_4/O_2/H_2O$ at RR = 2 and T_{in} = 400 K.

has a slower and less sharp peak and a wider distribution than that in N_2-dilution environment, as shown in Fig. 9a. It appears that H_2O-dilution reduces and retards the methane flame reactions through some chemical reaction steps related to the presence of the H_2O-dilution. Regarding to H_2 formation, hydrogen has an obvious peak production rate and a rapid follow-up consumption in the reaction zone in the N_2-dilution environment. The production rate of CO is higher than that of H_2 in the upstream section of reaction zone, but the consumption rate of CO is less than that of H_2 in the downstream section of reaction zone. In H_2O-dilution environment the production and consumption rates of H_2 and CO are certainly equal in the reaction zone. It is noted that the consumption of H_2 in downstream reaction zone is scarce, so it is the reason of hydrogen concentration enhancement in H_2O-dilution environment. Fig. 9b shows that the production and consumption rates of the H radical in H_2O-dilution environment is apparently less pronounced and slower than that in N_2-dilution environment, whereas the rate of OH radical consumption in H_2O-dilution environment is similar to that in N_2-dilution environment but slower. The maximum production and consumption rate of H and OH radical in H_2O-dilution environment shifts downstream compared to N_2-dilution environment. However, the ratio of H reaction rate to OH reaction rate in H_2O-dilutioin environment is smaller than that in N_2-dilution environment. The shift of maximum production rate on species and radicals is primarily caused by the change of flame temperature, but the difference on ratios of H/OH reaction rate is induced by radical competition. It is anticipated that the mechanism of H radical consumption and production are inhibited by the participation of H_2O diluent gas in chemical reactions.

In order to look further into the interplay of radical competition, Fig. 10 shows some net reaction rates of oxy-methane combustion related to methane consumption and hydrogen formation in N_2- and H_2O-dilution environments at the location of flame front. H and OH radicals consume methane mainly through R53 and R98 and recombin through R52. In the N_2-dilution case the rate of R53 is higher than that of R98, whereas the opposite occurs in the H_2O-dilution case. It appears that OH radcial promotes the inital consumption of methane in H_2O-dilution environment, but the main routes of methane consumption mechansim are analogous to those in N_2-dilution environment. Nevertheless, H_2O can also act as a thrid body and accelerate the recombunation rate of methane through R52. It contributes to attenuate the methane consumption. Regarding hydrogen formation, R53 is mainly contributed to H_2 production, and R84 is the main H_2 consumption step in the reaction zone for both dilution cases. R99 contributes to CO consumption via the assistance of OH radical. It is obvious that rate of R84 is higher than that of R53 and R99 in the N_2-dilution case, but the rate of R84 reduces to approximately equal to rates of R53 and R99 in the H_2O-dilution case. It demonstrates that the rate of H_2 consumption in the H_2O-dilution environment is relatively decreased, while the rate of CO consumption is relatively increased. It elucidates the trend of increasing hydrogen concentration and decreasing carbon monoxide concentration in the H_2O-dilution case compared to the H_2O(A)-dilution and N_2-dilution cases.

Fig. 11 shows some net reaction rates of oxy-methane combustion related to H and OH radical reactions in N_2- and H_2O-dilution environments at the location of flame front. In the H_2O-dilution environment, the main chain branching reactions of OH radical production are through R38 and R86 ($O + H_2O$═2OH), while main reactions of H radical production are through R84 and R166. The dominant step of OH radical production rate is R38, whereas the rates of R84 and R166 in H radical production are of equal importance. The presence of H_2O in oxy-methane combustion advances the reaction rate of R86 and R166. R166 becomes the main reaction step of H radical production, while R86 not only is the main provider of OH radicals, but also is the main H_2O consumption reaction. The exsitence of H_2O in the preheat zone results in enhancement of R35 ($O_2 + H + H_2O$═$HO_2 + H_2O$) step yielding large amounts of HO_2 radical, and it causes the competition for H radical among R35, R38 and R52. It is not doubted that the radical competition leads to reducing the reaction rate of R38, and further decreasing the O and OH radical productions. It is one of the main reason casuing the reduction of flame speed.

The ratio of H and OH radical concentration in H_2O-dilution environment is less than that in N_2- and H_2O(A)-dilution environments. This situation prompts enhancement of the rates of OH-related reaction, such as R98, R99, R101, R148 ($CH_2(S) + H_2O$═$CH_2 + H_2O$) and R166. Fig. 12 summarizes the simplified methane oxidation mechanism in the H_2O-dilution oxy-fuel environment. The difference between Figs. 6 and 12 is the enhancement of OH-related reactions in H_2O-diluent oxy-methane mechanism.

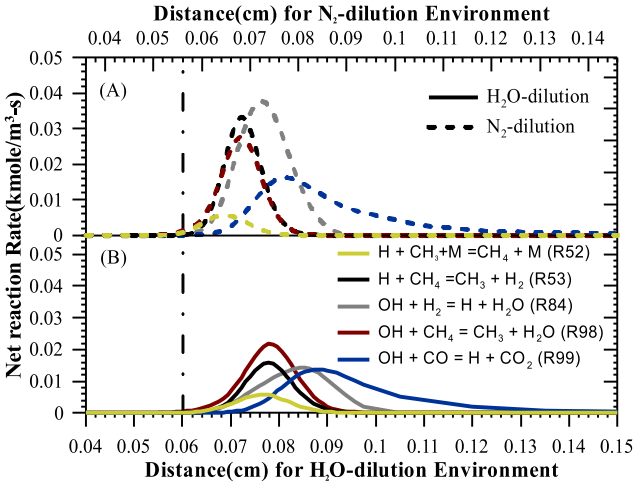

Fig. 10. The net reaction rate of (a) $CH_4/O_2/N_2$ and (b) $CH_4/O_2/H_2O$ at RR = 2 and T_{in} = 400 K.

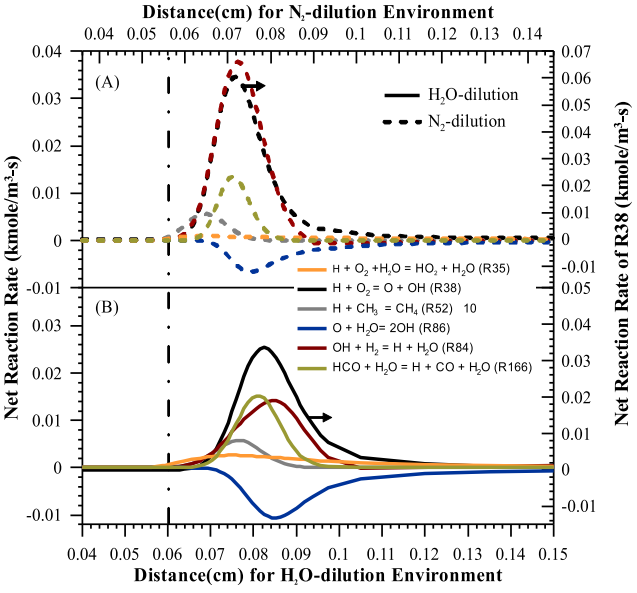

Fig. 11. The net reaction rate of (a) $CH_4/O_2/N_2$ and (b) $CH_4/O_2/H_2O$ at RR = 2 and T_{in} = 400 K.

3.3.3. CO_2-dilution oxy-methane flame

Fig. 13 shows the profiles of main species and radical concentrations along the axial direction in CO_2(A)- and CO_2-dilution oxy-methane flames at 400 K of gas temperature and RR = 2. The distributions of species and radical concentrations in CO_2(A)-dilution are similar to those in the N_2-dilution case (see Fig. 5), but values of the flame temperature as well as species and radical concentrations are different as only thermal effect of diluent gas is concerned. Comparing the profiles of species and radical concentrations between CO_2(A)- and CO_2-dilution environments, it is obvious to find a notable increase of CO concentration in both preheat and reaction zones of the CO_2-dilution case. The locations of flame front are seemingly identical; however, the location for the CO_2-dilution case shifts downstream slightly. For H_2 distribution, there is an apparent increase in the preheat zone for the CO_2-dilution case, and this trend becomes smoother after entering reaction zone. However, the quantity of H_2 concentration is much less than that for the CO_2(A)-dilution case. The radical concentrations, such as O, H, OH, HO_2 and CH_3, decrease in the CO_2-dilution environment, especially for the H radical concentration.

Fig. 14 shows the production rates of the main species and radicals along the axial direction in the N_2- and CO_2-dilution environments at the location of flame front. In Fig. 14a, the methane consumption rate for the CO_2-dilution case is slower than that for the N_2-dilution case. It seems that the methane consumption is restrained and retarded. Besides, the rate of H_2 production is much smaller than that of CO production in the CO_2-dilution case as compared with the N_2-dilution case. In addition, CO consumption rate is significantly reduced in CO_2-dilution case. The inception of CO_2 production is postponed until downstream of the reaction zone when compared with the N_2-dilution case. In Fig. 14b the H radical production and consumption rates in the CO_2-dilution case apparently decrease and become comparable to that of the OH radical. It demonstrates that the presence of CO_2 in the dilution gas would inhibit the consumption of CH_4 and CO and the production of H_2 and H radical, leading to the change of flame structure in the CO_2-dilution environment.

Fig. 15 shows the net reaction rates of oxy-methane combustion related to methane consumption and hydrogen formation in the N_2- and CO_2-dilution environments. For the CO_2-dilution case contribution to methane decomposition through R53 is becoming less important than that through R98. It appears that OH radical takes the role of primary methane decomposition in the CO_2-dilution environment, unlike H radical in the N_2-dilution environments. In the same time, R53 is also the primary hydrogen production mechanism. It appears that low H radical concentration in the CO_2-dilution environment contributes to the reduction of

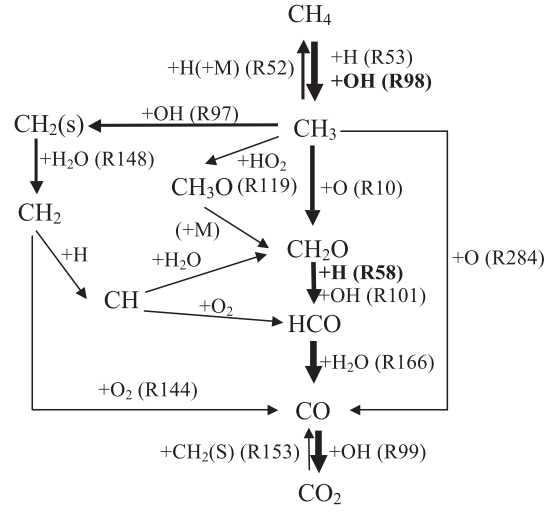

Fig. 12. Simplified methane oxidation mechanism in H_2O -dilution oxy-fuel environment.

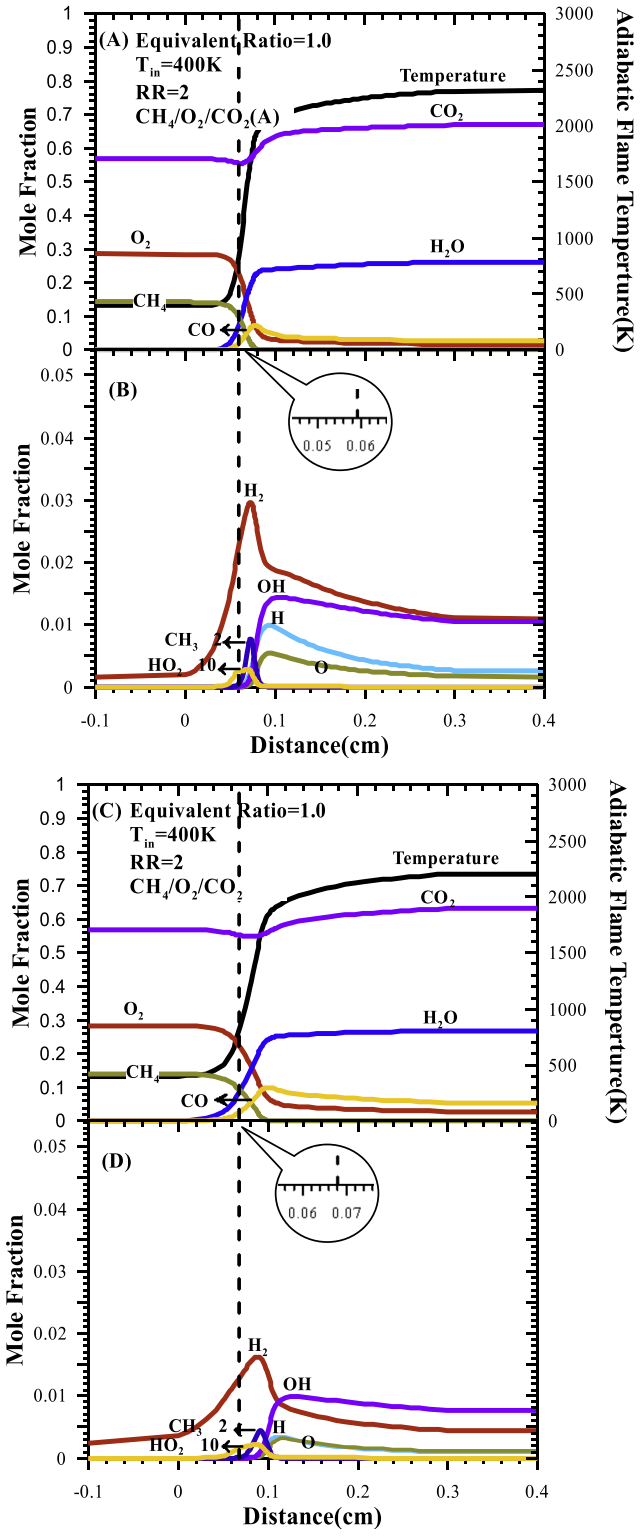

Fig. 13. Species concentration distribution of (a, b) $CH_4/O_2/CO_2$(A) and (c, d) $CH_4/O_2/CO_2$ at RR = 2 and Tin = 400 K.

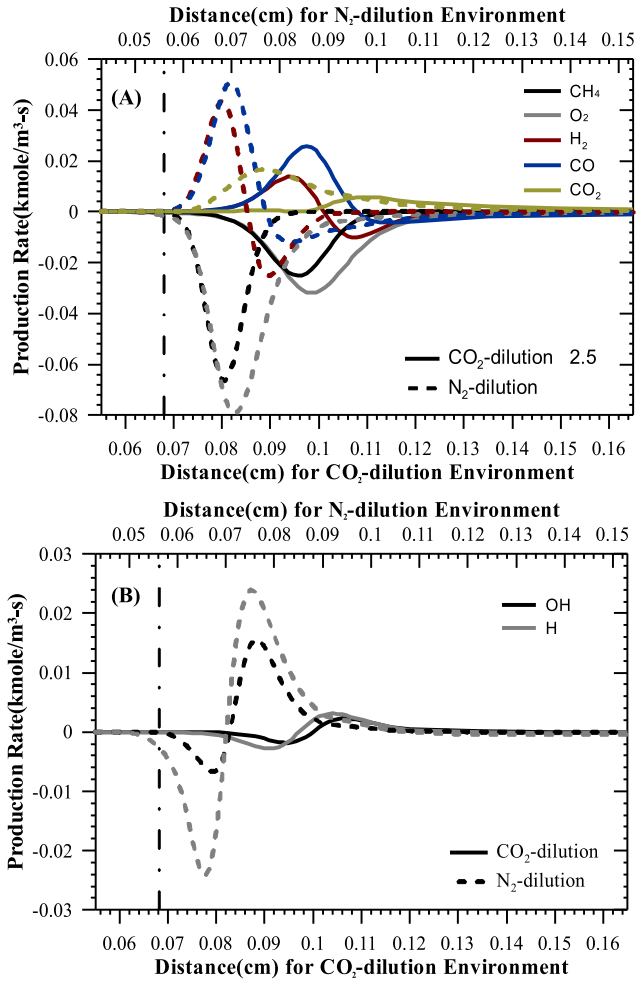

Fig. 14. The production rate of species and radical of $CH_4/O_2/N_2$ and $CH_4/O_2/CO_2$ at the RR = 2 and Tin = 400 k.

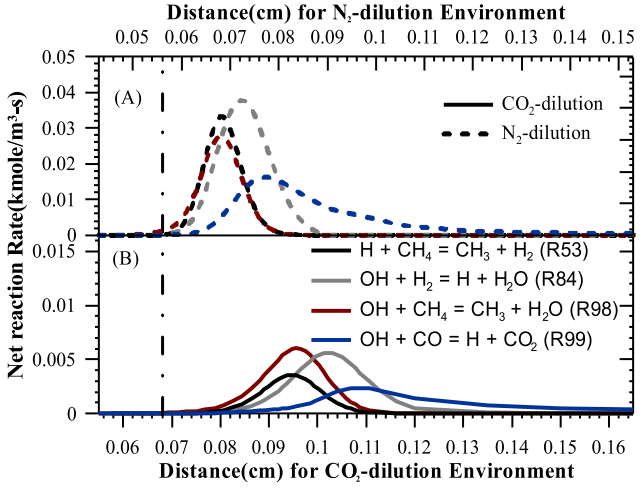

Fig. 15. The net reaction rate of (a) $CH_4/O_2/N_2$ and (b) $CH_4/O_2/CO_2$ at RR = 2 and T_{in} = 400 K.

hydrogen production. The ratio of H and OH radical concentrations for the CO_2-dilution case is much less than that for the N_2- and H_2O-dilution cases. It is imperative to examine the corresponding chemical reactions of H radical in the CO_2-dilution environment.

Fig. 16 shows the reaction rates of H radical in the N_2- and CO_2-dilution environment. The main reaction of H radical production is through R84, whereas the main reactions of H radical consumption are through R38, R52 and reverse reaction of R99. R84 is the main H_2 consumption reaction in methane combustion, releasing sufficient amounts of H radicals. R38 is main chain branching reaction, and R52 is the recombination of CH_3 with H radical which inhibits methane consumption. The reverse reaction of R99 is the decomposition of CO_2 with H radicals. Comparing the reaction for the two dilution cases, the R84 reaction decreases in the downstream region of the reaction zone, but the reverse reaction of R99 significantly increases for the CO_2-dilution case. The influence of R52 becomes more pronounced in the CO_2-dilution case, and it is the main inhibition step of methane consumption. It is one of the primary reasons that the methane consumption rate in the CO_2-dilution is retarded, as shown in Fig. 14a. Furthermore, it is also noted that CO_2 penetrates in the reaction zone, and reacts with H radicals to yield CO through the reverse reaction of R99. The competition for the H radical between R99 and R38 becomes significant and competitive in the reaction zone of the CO_2-dilution flame. It leads to reduction of the reaction rate of R38, and decrease of the production of O and OH radicals. It further reduces the rate of R84 by decreasing the supply of OH radicals.

Fig. 17 summarizes the simplified methane oxidation mechanism in the CO_2-dilution oxy-fuel environment. H and OH radicals trigger methane initial decomposition through R53 and R98, but the rate of R98 is significantly higher than that of R53 in CO_2-dilution oxy-methane combustion. The route of methane consumption through R97 is dominant and slightly higher than that through R10 in the N_2-dilution environment. The dominant reaction of CH_2O consumption is R101 ($OH + CH_2O = HCO + H_2O$), and is slightly higher than that of R58 in the N_2-dilution environment. HCO, similar to chemical reactions in the N_2-dilution environment, is mainly consumed through R166 ($HCO + H_2O = H + CO + H_2O$), and CO is consumed through R99 ($CO + OH = CO_2 + H$) and eventually yeilds CO_2. However, it is of interest to note that the reaction

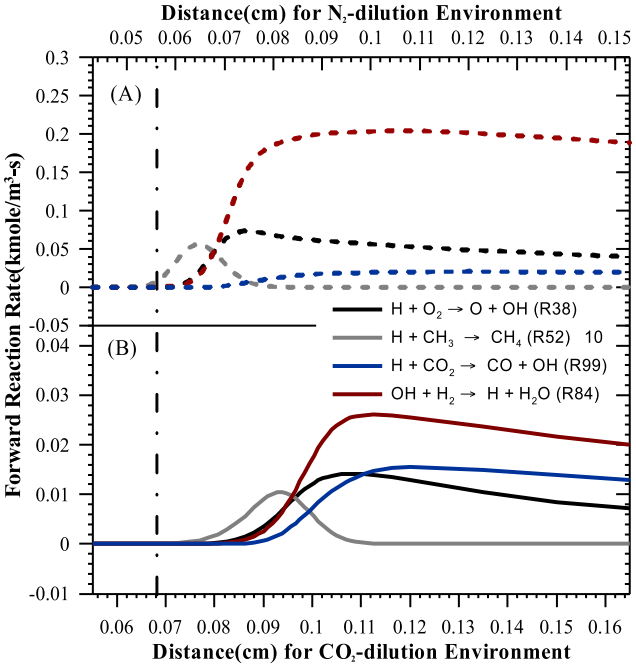

Fig. 16. The forward reaction rate of H radical formation in (a) $CH_4/O_2/N_2$ and (b) $CH_4/O_2/CO_2$ at RR = 2 and T_{in} = 400 K.

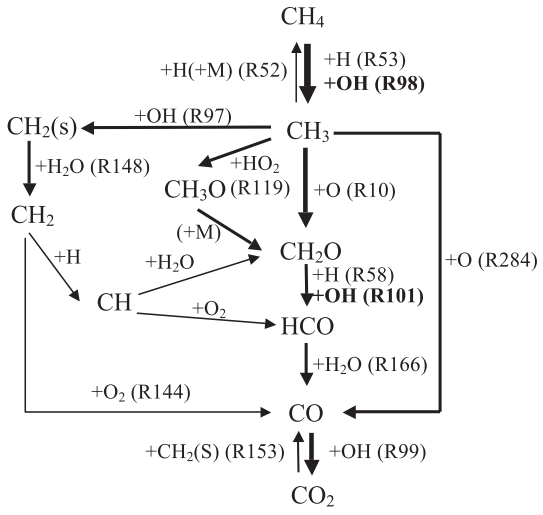

Fig. 17. Simplified methane oxidation mechanism in CO_2 -dilution oxy-fuel environment.

of CO_2 consumption or CO production through R153 ($CH_2(S) + CO_2$=$CO + CH_2O$) is apparently increased. In the summary, it has found that the dominant reaction of CH_4 consumption is changed to R98 in the CO_2-dilution environment. CH_4 tends to oxidize with OH radical and so do CH_3 and CH_2O. The existence of CO_2 enhances the reverse reaction rate of R99. The reverse reaction of R99 will compete with R38 for H radicals. The reaction rate of R38 is decreased due to the limited supply of free H radicals, and the prodution of O and OH is obviously decreased. Then, the reaction rate of R84 is decreased due to the reduction of OH radical. In addition, the CO_2-dilution environment also enhances the reaction rate of R153,. resulting in a decrease of the CO_2 concentration but an increase of the CO concentration.

3.3.4. *Fluegas-dilution oxy-methane flame*

Compared with the fluegas(A)-dilution case as shown in Fig. 18, species and radical concentrations in the fluegas-dilution case such as CH_3, H and O, are seen to decrease, and such as H_2, OH and HO_2 slightly increase. Nonetheless, the intermediate species CO is of no significant difference in these two dilution cases. It appears that the change of main species and radical concentrations in the flue gas dilution environment has the root and acts as the combination of the changes in the H_2O- and CO_2-dilution cases discussed above. Similarly, the location of flame front in the fluegas-dilution case is also seen to shift downstream as compared to that in the fluegas(A)-dilution case. Comparing the main chemical reactions of methane consumption and hydrogen formation in N_2- and fluegas-dilution environments as shown in Fig. 19, it is noted that R98 reaction is the dominant step in initial methane decomposition for the fluegas-dilution case due to the increasing amount of OH radical. The change of hydrogen formation in the fluegas-dilution case is not pronounced, but CO consumption through R99 is relatively increasing due to abundant OH radical compared to R84.

Fig. 20 shows some important chemical reactions in N_2- and fluegas-dilution environments. Results indicate the reaction rates of R5, R86 and R166 increase due to the effect of water steam in the flue gas, and in the meantime the reaction rate of R153 also slightly increases due to the effect of carbon dioxide in the flue gas. It is noted that the dominance of the effect of the water steam over that of carbon dioxide results from the composition of 33% CO_2 and 67% H_2O in the flue gas. Furthermore, R38 has evident reduction in the flue gas dilution environment compared to that in the N_2-dilution

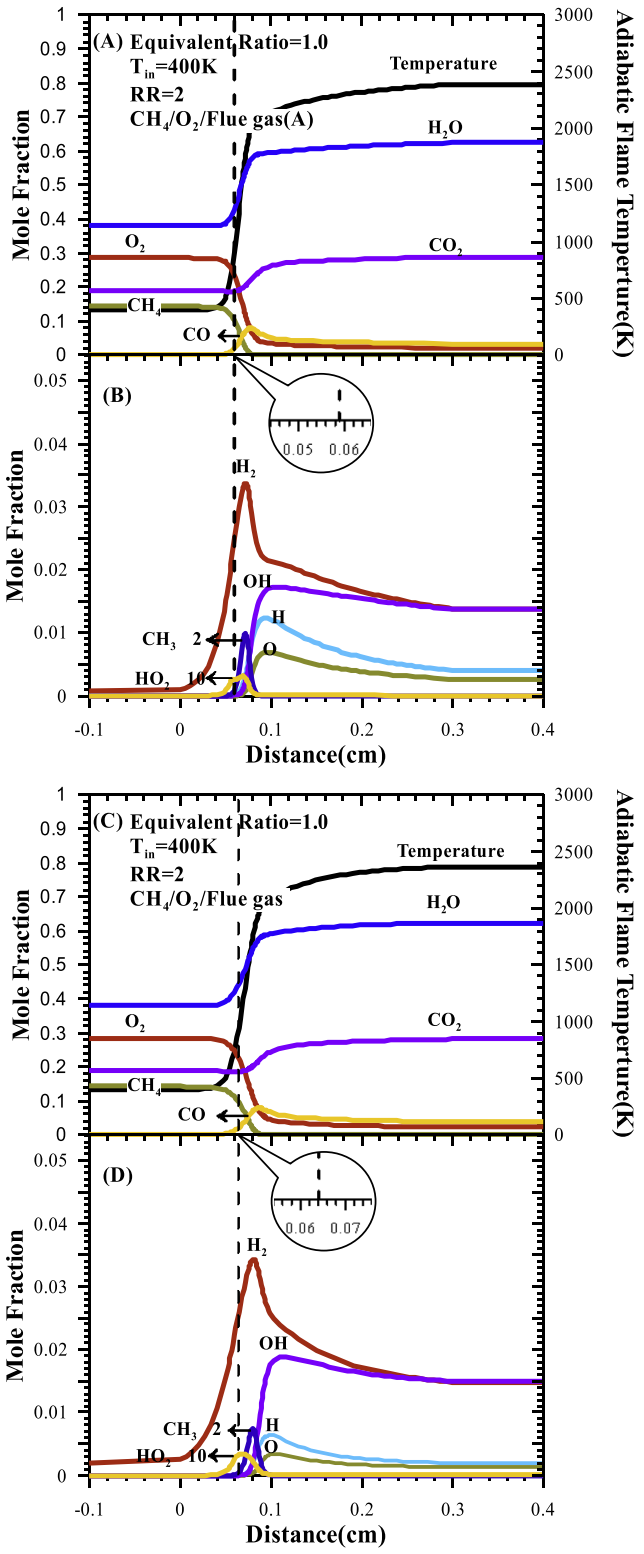

Fig. 18. Species concentration distribution of (a, b) CH_4/O_2/Fluegas(A) and (c, d) CH_4/O_2/Fluegas at RR = 2 and T_{in} = 400 K.

environment. R38 has to compete for H radicals with other H-related chemical reactions, such as R35, R52 and R99. Besides, OH radical induced from H_2O enrichment can facilitate CO consumption through R99 as shown in Fig. 18, and it results in prohibition of CO production in the reaction zone, dissimilar to an abundant CO

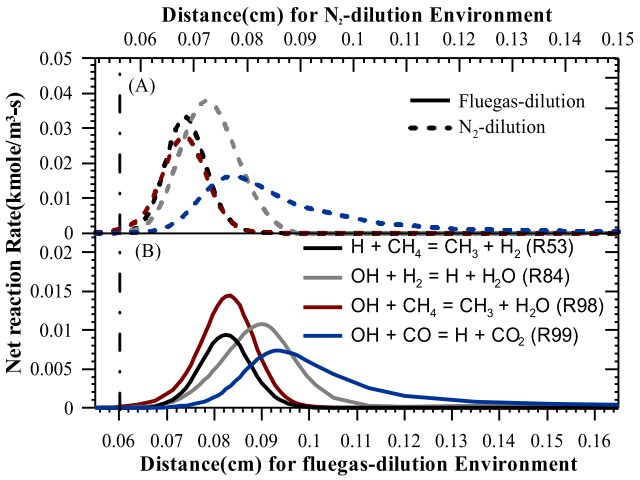

Fig. 19. The net reaction rate of (a) $CH_4/O_2/N_2$ and (b) CH_4/O_2/Fluegas at RR = 2 and T_{in} = 400 K.

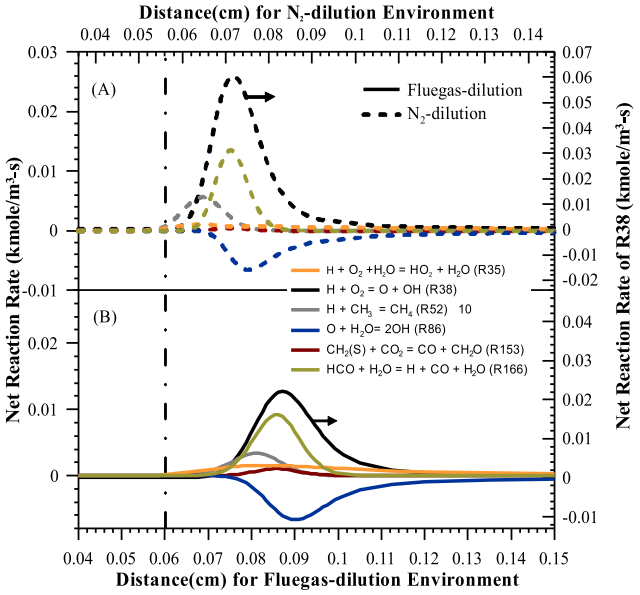

Fig. 20. The net reaction rate of (a) $CH_4/O_2/N_2$ and (b) CH_4/O_2/Flue gas at RR = 2 and T_{in} = 400 K.

production in the CO_2-dilution environment. Fig. 21 shows the simplified methane oxidation mechanism in fluegas-dilution oxy-fuel environment.

4. Conclusions

The oxy-fuel combustion using recirculated carbon-dioxide as diluents may behave differently with the traditional air combustion with nitrogen as the diluents. The difference in physical and chemical properties between carbon-dioxide and nitrogen may result in different combustion and flame phenomena. However, the content of carbon-dioxide and water steam in the flue gas not only has thermal effects on combustion, but also changes chemical reaction in the flame. The chemical effects on oxy-fuel combustion have not been intensively studied and discussed so far. Thus, in this study we focus on the chemical effects of the recirculated fluegas oxy-fuel combustion by using numerical simulation and comparing with the results using fictitious chemically-inert gases CO_2(A) and

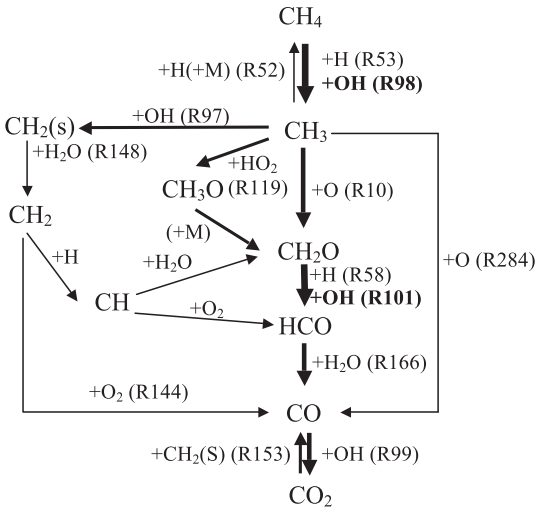

Fig. 21. Simplified methane oxidation mechanism in Fluegas -dilution oxy-fuel environment.

H_2O(A) for further analysis of the chemical effects on flame structure and flame characteristics. Laminar burning velocity is the crucial parameter for premixed flame, which is the major flame characteristic expressing the burning intensity. Therefore, in this study we first use a conical flame to measure laminar flame speed for comparison and validate the numerical simulation results. The results show that the discrepancy is within in 1.5%.

The simulation results show that adiabatic flame temperature and laminar burning velocity gradually decrease with increasing concentration of added gas N_2, H_2O and CO_2 into oxygen/methane flame. In contrast, the numerical results of adiabatic flame temperature of the added the fictitious diluent gas CO_2(A) and H_2O(A) as compared with the real gases H_2O and CO_2 have little difference. On the other hand, the laminar burning velocity has significant variation, it indicates that chemical effects of the recirculated gases do change the combustion characteristics significantly in terms of the burning velocity.

By observing the resultant flame temperature and species concentration profiles one can identify that the flame front shifts, and the concentration profile of major chemical reaction radicals varies, indicating the change of flame structure and flame chemical reaction paths. The dominant initial consumption reaction step of methane shifts from R53 to R98 when nitrogen is replaced by the recirculated gases. It is because that the reduction of H radical concentration and increase of OH radical concentration results in the chemical reaction shaft on methane decomposition in oxy-combustion.

In the case of H_2O-dilution, the chemical reaction rate of R52 has been increasing due to aboundant H_2O acting as third body, and it leads to the reduction of initial methane decompostion. Besides, R38 is primary chemical reaction affacting the flame speed based on sensitivity analysis. However, the competition of H radical between R38 and other chemical reactions, such as R35 and R52, so that it leads to the reducation of radical provision through R38. However, R86 and R166 can are primary chemical reactions to provide sufficient H and OH radical and to trigger successive chemical reactions. In the case of CO_2-dilution, R38 is still a primary chemical reaction based on sensitivity analysis of flame speed. Nevertheless, the effect of R99 has been evoking and struggling for H radical competed with R38. The reduction of chemical reaction rate on R38 results into the influence of successive chemical oxidation reaction. In the case of flue gas dilution, the influence of dilution effect superposes the effect of carbon dioxide and water

steam in oxy-fuel combustion. The competition of H radical among R35, R38, R52, and R99 is analogously occurred. However, the content of water steam is larger than that of carbon dioxide in flue gas, so that the effect of water steam is mainly contributed to the changes on chemical reaction of oxy-fuel combustion.

Acknowledgments

This research was partially supported by the Ministry of Science and Technology (Republic of China) under Grant numbers MOST 104-2218-E-006-012. Computer time and numerical packages provided by the National Center for High-Performance Computing, Taiwan (NCHC Taiwan), are gratefully acknowledged.

References

[1] Buhre BJP, Elliott LK, Sheng CD, Gupta RP, Wall TF. Oxy-fuel combustion technology for coal-fired power generation. Prog Energy Combust Sci 2005;31:283–307.
[2] Chen L, Yong SZ, Ghoniem AF. Oxy-fuel combustion of pulverized coal: characterization, fundamentals, stabilization and CFD modeling. Prog Energy Combust Sci 2012;38:156–214.
[3] Liszka M, Ziębik A. Coal-fired oxy-fuel power unit – process and system analysis. Energy 2010;35:943–51.
[4] Horbaniuc B, Marin O, Dumitras G, Charon O. Oxygen-enriched combustion in supercritical steam boilers. Energy 2004;29:427–48.
[5] Molina A, Shaddix CR. Ignition and devolatilization of pulverized bituminous coal particles during oxygen/carbon dioxide coal combustion. Proc Combust Inst 2007;31:1905–12.
[6] Wang CS, Berry GF, Chang KC, Wolsky AM. Combustion of pulverized coal using waste carbon dioxide and oxygen. Combust Flame 1988;72:301–10.
[7] Kimura K, Omata K, Kiga T, Takano S, Shikisima S. Characteristics of pulverized coal combustion in O_2/CO_2 mixtures for CO_2 recovery. Energy Convers. Manage 1995;36:805–8.
[8] Ditaranto M, Hals J. Combustion instabilities in sudden expansion oxy-fuel flames. Combust Flame 2006;146:493–512.
[9] Riaza J, Alvarez L, Gil MV, Pevida C, Pis JJ, Rubiera F. Effect of oxy-fuel combustion with steam addition on coal ignition and burnout in an entrained flow reactor. Energy 2011;36:5314–9.
[10] Payne SLCR, Wolsky AM, Richter WF. CO_2 recovery via coal combustion in mixtures of oxygen and recycled flue gas. Combust Sci Technol 1989;67:1–16.
[11] Halter F, Foucher F, Landry L, Mounaim-Rousselle C. Effect of dilution by nitrogen and/or carbon dioxide on methane and iso-octane air flames. Combust Sci Technol 2009;181:813–27.
[12] Liu F, Guo H, Smallwood GJ. The chemical effect of CO_2 replacement of N_2 in air on the burning velocity of and premixed flames. Combust Flame 2003;133:495–7.
[13] Glarborg P, Bentzen LLB. Chemical effects of high CO_2 concentration in oxy-fuel combustion of methane. Energy Fuels 2008;22:291–6.
[14] Park J, Hwang DJ, Kim KT, Lee SB, Keel SI. Evaluation of chemical effects of added CO_2 according to flame location. Int J Energy Res 2004;28:551–65.
[15] Mazas AN, Fiorina B, Lacoste DA, Schuller T. Effects of water vapor addition on the laminar burning velocity of oxygen-enriched methane flames. Combust Flame 2011;158:2428–40.
[16] Watanabe H, Yamamoto J, Okazaki K. Nox formation and reduction mechanisms in staged O_2/CO_2 combustion. Combust Flame 2011;158:1255–63.
[17] Watanabe H, Arai F, Okazaki K. Role of CO_2 in the CH_4 oxidation and H_2 formation during fuel-rich combustion in O_2/CO_2 environments. Combust Flame 2013;160:2375–85.
[18] Mendiara T, Glarborg P. Ammonia chemistry in oxy-fuel combustion of methane. Combust Flame 2009;156:1937–49.
[19] Abián M, Gimnez-López J, Bilbao R, Alzueta MU. Effect of different concentration levels of CO_2 and H_2O on the oxidation of CO: experiments and modeling. Proc Combust Inst 2011;33. 137–123.
[20] Glarborg P, Alzueta MU, Dam-Johansen, Miller KJA. Kinetic modeling of hydrocarbon/nitric oxide interactions in a flow reactor. Combust Flame 1998;115:1–27.
[21] Bowman C, Hanson T, Davidson DF, Gardiner WC, Lissianski V, Smith GP, Golden DM, Frenklach M, Goldenberg M. http://www.me.berkeley.edu/gri_mech/.
[22] Kee RJ, Rupley FM, Meeks E, Miller JA. Report No. SAND96–8216. Sandia National Laboratories; 1996.
[23] Law CK, Sung CJ. Structure, aerodynamics, and geometry of premixed flamelets. Prog Energy Combust Sci 2000;26:459–505.
[24] Oh J, Noh D. Laminar burning velocity of oxy-methane flames in atmospheric condition. Energy 2012;45:669–75.
[25] Bouvet N. Characterization of syngas laminar flames using the Bunsen burner configuration. Int J Hydrog Energy 2011;36:992–1005.
[26] Sun CJ, Sung CJ, He L, Law CK. Dynamics of weakly stretched flames: quantitative description and extraction of global flame parameters. Combust Flame 1999;118:108–28.
[27] Chen GB, Li YH, Cheng TS, Chao YC. Chemical effect of hydrogen peroxide addition on characteristics of methane-air combustion. Energy 2013;55:564–70.
[28] Normann F, Andersson K, Johnsson F, Leckner B. Reburning in oxy-fuel combustion: a parametric study of the combustion chemistry. Ind Eng Chem Res 2010;49:9088–94.